Biogeosciences Discuss., 6, 4993–5030, 2009
www.biogeosciences-discuss.net/6/4993/2009/

Biogeosciences Discussions

Biogeosciences Discussions is the access reviewed discussion forum of *Biogeosciences*

Hydrodynamics and light climate structure alongshore phytoplankton blooms in spring

G. Brandt and K. W. Wirtz

GKSS-Research Centre, Institute for Coastal Research, Max-Planck-Str. 1, 21502 Geesthacht, Germany

Received: 26 April 2009 – Accepted: 28 April 2009 – Published: 13 May 2009

Correspondence to: G. Brandt (brandt@bpt-info.de)

Published by Copernicus Publications on behalf of the European Geosciences Union.

Abstract

Phytoplankton blooms are a recurring phenomenon that have significant impact on annual biogeochemistry and food-web dynamics in many aquatic ecosystems. The causes for their variability, which is high especially in coastal seas, remain poorly understood. We present an example for distinct differences in the spatio-temporal chlorophyll-*a* (CHL-*a*) distribution on an interannual scale, integrating high-frequency data from an autonomous measuring device (FerryBox), which operated on an alongshore route in the coastal North Sea. While in one year CHL-*a* was spatially homogeneous (2004), a bloom only developed in one part of the transect in the following spring period (2005). In this study, we use a one-dimensional Lagrangian particle tracking model, which operates along the mean current direction, combined with a NPZ-model to identify the mechanisms controlling interannual bloom variability on an alongshore transect. The model results clearly indicate that in 2004, the local light climate triggered phytoplankton growth, whereas in the following year, advective transport determined the spatial structure of the spring bloom. A pronounced eastward inflow event in 2005 imported a high CHL-*a* patch into the western half of the study area from the adjacent Southern Bight. It did, however, not last long enough to also spread the bloom into the eastern part, where high turbidity prevented local phytoplankton growth. The model identified two interacting mechanisms, light climate and hydrodynamics that control the alongshore dynamics. Especially the occurrence of a pronounced spring bloom despite unfavourable light conditions in 2005 underlines the need to carefully consider hydrodynamics to understand ecosystem functioning in coastal environments.

1 Introduction

The phytoplankton spring bloom drives food web dynamics and matter cycling in most temperate aquatic ecosystems (Sommer, 1998). Despite its recurrence, the timing, the spatial extent, and the duration of the first seasonal peak in algal concentration

BGD

6, 4993–5030, 2009

show considerable interannual variation. While in deep waters the onset of a bloom typically follows stratification in spring, in shallow coastal seas interannual variability and spatial heterogeneity are particularly strong (Thomas et al., 2003; Cloern, 1996). Only the magnitude of the bloom seems to be predictable as a function of winter nutrient concentration (Loebl et al., 2009; Muylaert et al., 2006; Cloern, 1996). Before and during the bloom event, however, the balance between algal production and loss in near-shore waters is sensitive to a multitude of different factors such as temperature, water transparency, abundance of herbivores, stratification, or incident irradiance. Thus, observed irregularities mainly reflect the sensitivity of spring bloom development to fluctuating physical and, to a lesser extend, biological conditions of which turbidity and benthic grazing are typically considered to be most important (Cloern, 1996). Turbulence, generated by wind- or tide-induced currents, affects both factors: It decreases light availability for phytoplankton by enhancing turbidity, which is suggested to be pivotal for phytoplankton bloom control (Townsend et al., 1994), and strengthens vertical mixing. The latter also increases mortality because of grazing by benthic filter-feeders Cloern (1996); Prins et al. (1996). Mixing is, however, not always retarding blooms (Iriarte and Purdie, 2004) underlining the importance of other site-specific mechanisms such as freshwater induced stratification, resuspension of benthic diatoms, or species composition. The range of potential mechanisms considerably complicates the establishments of general rules for biological responses to various physical forcings.

Strong horizontal advection, which in coastal seas is usually connected to winds and tides, links temporal variability to spatial gradients. Advection also translates local growth or loss to commonly observed patchiness in phytoplankton distributions (Martin, 2003). Lucas et al. (2009, 1999b) have shown how lateral transport from a productive area can result in chlorophyll-*a* (CHL-*a*) accumulation in an adjacent deep and unproductive channel proposing that spatial structures are either of local origin or a consequence of variable transport. Apart from the studies of Lucas et al. (1999a,b) in a shallow estuary, little is known about the interaction of advection with spatio-temporal variability in phytoplankton growth at intermediate to larger scales.

In the North Sea, Levin (1992) documented patchiness in CHL-*a* along a 5 to 10 km latitudinal transect. In the last two decades, satellite imagery has added a wealth of data on phytoplankton blooms around the globe and has proven to be a useful tool to enhance the understanding of ecosystem function. In temperate coastal seas and especially in the North Sea, however, high cloudiness strongly restricts the availability of data and often prevents the use of satellite imagery to detect fast biological dynamics on a scale of only a few days.

High-frequency and time-continuous measurements by autonomous systems installed on ferries are filling this gap since recently. These FerryBoxes enable physical, chemical and biological observations along the one-dimensional tracks of a growing number of ships of opportunity, mostly sailing in European waters (Ainsworth, 2008). Data from a FerryBox operating on the route between Cuxhaven, Germany and Harwich, UK, reveal intense mesoscale patterns in CHL-*a* (Petersen et al., 2008). Bloom development in the English Channel as well as along the continental coast significantly differed in timing, location, and magnitude from 2004 to 2005.

Mesoscale patchiness (1 to 100 km) is a property of phytoplankton distributions, which still challenges state-of-the-art ecosystem models. Coupled physical–biogeochemical models for the North Sea reproduce typical cross-shore gradients in CHL-*a* in the Southern Bight (Lacroix et al., 2007) or the German Bight (Tian et al., 2009), but fail to reproduce prominent characteristics observed in time-series or FerryBox data. Despite high-frequency physical forcing and narrow grid spacing, these models are not able to generate significant alongshore variability and sharp temporal gradients. One reason for this limited capability is that in coupled ecosystem models lateral gradients in CHL-*a* are to a high degree determined by local factors. In the study of (Tian et al., 2009), for example, even the integration of (model-derived) turbidity fields did not lead to much increased spatio-temporal variability. This demonstrates that Eulerian ecosystem models, despite resolving mesoscale features of the circulation and spatially heterogeneous physical forcing, still tend to underestimate the variability of biological state variables in coastal seas.

We therefore apply a Lagrangian approach for simulating and understanding mesoscale dynamics in coastal spring blooms. For theoretical or educational purposes, Woods et al. (2005) introduced ensembles of "ecosystem tracers" advected by physical circulation. Developing further this concept, we use ensembles of Lagrangian ecosystems to study the origin of strong alongshore (i.e. isobath) gradients in net phytoplankton growth.

2 Study area

The study area is a section off the German and Dutch North Sea coast ranging from the Ijsselmeer in the West to the Elbe estuary in the East. It is limited by the Wadden Sea in the South and German Bight offshore waters in the North. Prevailing westerly winds (Siegismund and Schrum, 2001) and the counter-clockwise tidal wave result in an eastward mean current that closely follows the coastline (Staneva et al., 2009). Winds and tides also keep this shallow coastal sea with water depths below 40 m well mixed throughout most of the year. Several rivers (Fig. 1: Elbe, Weser, Ems, and Rhine through the Ijsselmeer) discharge into the German Bight supplying it with high nutrient loads (Beddig et al., 1997; Radach, 1992). Especially in the estuaries in the East, waters are highly turbid due to riverine suspended particulate matter. Waves and currents additionally enhance the resuspension of sediment from the soft bottom (Staneva et al., 2009) causing a steep turbidity gradient from the shore to the open sea. Water temperatures range from close to zero in winter to values exceeding 20°C during calm periods in warm summers (Wiltshire and Manly, 2004).

Phytoplankton in this region exhibits an articulate annual cycle with low winter production due to light limitation and low temperatures followed by a distinct spring bloom that is later terminated by nutrient limitation and grazing (Iriarte and Purdie, 2004). Often, a second phytoplankton bloom develops in late summer before light conditions prevent significant primary production. Thereafter, nutrients recover to maximum winter values (Loebl et al., 2009; Wiltshire et al., 2008).

3 Methods

3.1 Measured data

Most data presented in this study were measured by a FerryBox (Petersen et al., 2008, 2003) that was installed on a ferry sailing from Cuxhaven, Germany to Harwich, UK several times a week (Fig. 1). Here, the FerryBox variables temperature, turbidity and CHL-*a* are used. Irradiance data was obtained from a measurement pile in the Wadden Sea, which is located on the eastern edge of the study area (Fig. 1, www.coastlab.org). Nutrient data from the FerryBox are not considered because of the unsatisfactory data coverage in the study period and their uncertain quality. Instead, phosphate data from two stations in Dutch waters (5.10° E, 53.46° N and 5.15° E, 53.41° E) are used. See Appendix for more details.

3.2 Model architecture

An individual-based model describes the physical and ecological dynamics of the phytoplankton in the study area. While transport due to advective processes is simulated by a Lagrangian particle tracking model, the dynamics of nutrients N, phytoplankton P and zooplankton Z is accounted for by an ecosystem model, which runs in each particle.

Hydrodynamics in the German Bight are driven by prevailing westerly winds and semi-diurnal tides resulting in a dominant alongshore, i.e. north-easterly or south-westerly, current. This feature is relatively stable throughout the year and becomes evident from the analysis of currents generated by the General Estaurine Transport Model (GETM, Staneva et al., 2009; Stips et al., 2004), which is especially suited to simulate the hydrodynamics in tidally-dominated shallow seas (Fig. 3). Significant correlations between the horizontal current components motivated a projection of the two-dimensional flow field onto the mean axis of transport. In doing so, the model domain is reduced to a one-dimensional transect, while the general hydrodynamic properties

are preserved. Furthermore, vertical homogeneity is assumed, since the study area is shallow with depths between 25 and 35 m and the water column is well-mixed during the period of interest in spring. This is supported by Joint and Pomroy (1993), who found no chlorophyll gradients within the euphotic zone at most sites in the North Sea.

Particles are transported by a particle tracking model, which uses the zonal component u of the mean daily current velocity generated by GETM while the meridional component v is defined as a linear function of u (see Appendix). A Lagrangian particle, thus, moves along the one-dimensional transect shown in Fig. 1. The entire simulation then consists of an ensemble of particles with different initial conditions (for N, P and Z) and particle trajectories, which are subject to different physical forcings (temperature, turbidity and photosynthetically active radiation (PAR)).

3.3 Ecosystem model

Each particle carries a conceptualised ecosystem consisting of three compartments for one nutrient N, phytoplankton P and zooplankton Z. All variables are in phosphorus units. Primary production P_P is regulated by light following the approach of Ebenhöh et al. (1997). Furthermore, temperature and the availability of nutrients affect the production of phytoplankton biomass.

$$P_P = \mu_P \times TPT \times NPT \times LPT \times P \tag{1}$$

where μ_P denotes the maximum growth rate of phytoplankton and TPT, NPT, and LPT are the production terms of temperature, nutrients and light, respectively. P_P links the consumption of nutrients to the growth of phytoplankton, which is additionally subject to zooplankton grazing P_Z. Thus, the model system describing the dynamics of all three compartments is given by

$$\frac{\partial N}{\partial t} = -P_P \tag{2}$$

$$\frac{\partial P}{\partial t} = P_P - P_Z \tag{3}$$

$$\frac{\partial Z}{\partial t} = \beta \times P_Z \,, \tag{4}$$

with the zooplankton assimilation efficiency β. A more detailed model description is given in the Appendix. Because of the omission of detritus and, consequently, the remineralisation, the model systematically underestimates nutrient concentrations. To our understanding, this simplification is not critical in winter and spring, since the nutrient concentration remains above limiting levels during most of the simulation period.

4 Parametrisation, initial conditions and forcing

Every six hours a particle is released at 5.4° E during the first 20 weeks in 2004 and 23 weeks in 2005. Initial values for nutrient and phytoplankton concentrations are derived from measurements (Fig. 2). Phytoplankton biomass is converted from CHL-*a* data by means of two constant ratios. A Redfield C:P ratio and a Chl:C ratio of $0.3\,\mathrm{g\,CHL\text{-}}a \times (\mathrm{mol\,C})^{-1}$ are assumed. The latter is in agreement with several measurements in the southern North Sea (Llewellyn et al., 2005; Geider, 1987). These authors, however, also report a high variability in Chl:C and its dependence on several factors of which temperature, nutrient and light availability have been regarded to be most important (Taylor et al., 1997; Cloern, 1995). Similar effects are known for C:P (Elser et al., 2000; Klausmeier et al., 2004). Fixing the the Chl:P ratio, thus, implies a strong simplification, which introduces a significant uncertainty into the model. Zooplankton data are unavailable in the required spatial and temporal resolution. Instead, initial zooplankton biomass at the initial position x_0 is estimated as a fraction of the phytoplankton biomass at a previous time. During the first half of the year, the assumption of zooplankton lagging behind phytoplankton is well documented at the nearby time-series station of Helgoland roads (Greve et al., 2004). Later in the year, however, the zooplankton initialisation clearly loses its validity. After initialisation, the evolution of the three ecosystem variables is determined by the water depth ζ, the water temperature T, and the light climate. T and ζ are derived from FerryBox measurements and the

GETM bathymetrie, respectively. The light climate is calculated using hourly surface PAR I_0, which is derived from incident irradiance data from a measurement pile, and measured turbidity (Fig. 5, cf. Appendix).

Most parameter values have been manually calibrated within known ranges and according to literature values (Table 1). Four sensitive parameters (I_{opt}, k_N, k_P and Z_{min}) that were identified manually, however, are calibrated with the objective of (1) maximising the lateral CHL-*a* gradient along the transect in 2005, and (2) minimising the gradient in 2004 (cf. Fig. 4). Therefore, the simulated ratio of mean CHL-*a* in two neighbouring regions during spring bloom is calculated and compared to the same ratio derived from measurements.

5 Results

5.1 Measured spring bloom dynamics

A continuous spring bloom is observed by the FerryBox throughout the study area in 2004 (Fig. 5). Starting in the western part in week 12, a patch with CHL-*a* concentrations above 30 µg l^{-1} developed eastward within six weeks. Measured turbidity data, however, exhibit an inverse pattern (Fig. 5). While winter values fluctuated considerably between 2 and 10 FTU, the variability decreased throughout spring and values below 3 FTU indicate good light availability. The spatial and temporal extend of the minimum in turbidity closely resembles the pattern of maximum CHL-*a*. Parallel to turbidity, incident irradiances (not shown) supported the onset and decay of the bloom with already high values in week 12 and 13 and several days with relatively low values in week 19. Low temperatures did not prevent the growth of phytoplankton, as the onset of the spring bloom around week 12 in 2004 coincided with the coldest period in this year (Fig. 2). Thereafter, temperature was steadily rising as was CHL-*a*.

Though phosphate data are relatively sparse compared to FerryBox measurements, it nonetheless outline the high temporal dynamics of phosphate during the spring

(Fig. 2). After a steep decrease from winter values phosphate concentrations already marked a turning point around week 15, which was followed by a significant recovery until week 20. Phosphate concentration started to decrease from winter values of 0.7 µmol l^{-1} between week 10 and 12, marked a low in week 15, and recovered until the end of the period considered in this study (week 20).

In 2005, an articulate bloom with CHL-*a* above 20 µg l^{-1} only occurred in the western part of the study area (Fig. 5). Measured CHL-*a* rarely exceeded 5 µg l^{-1} further east between 6.4° E and 7.5° E. Unlike in 2004, patterns of high chlorophyll concentrations were associated with high turbidity in 2005 and the minimum of turbidity already occurred before the onset of the spring bloom between week 12 and 15. After phosphate concentrations decreased slightly during the initial phase of the bloom, exceptionally high values exceeding 3 µmol l^{-1} were measured during the maximum of the bloom in week 18 (Fig. 2).

5.2 Sensitivity analysis

A systematic variation of the four parameters I_{opt}, k_N, k_P and Z_{min} (Table 1) reveals considerable robustness of the obtained CHL-*a* patterns with respect to uncertain parameters. While absolute values of CHL-*a* are strongly depending on the parametrisation, the ratio of CHL-*a* concentrations in two zonally adjacent areas turned out to be rather consistent (see Fig. 5 for the definition of the areas) indicating that different mechanisms were dominant in each of the years.

In 2004, there is no spatial gradient in the measured data and the simulations reveal a mean ratio close to 0.7, i.e. slightly higher CHL-*a* values in the West than in the East (Fig. 4). In the following year, the measured ratio indicates distinctively higher CHL-*a* concentrations in the West than in the East and the simulations resemble that relation with a mean value below 0.4. Values that are distinctively higher than the mean have not been obtained in the systematic sensitivity study. The selected reference parametrisation given in Table 1 is not optimal for reproducing the CHL-*a* data in each of the years, but presents a compromise to simulate qualitatively different phytoplankton

dynamics in two consecutive years with a constant set of parameters. Following model results have been produced with this reference parameter set.

5.3 Bloom control by light climate in 2004

The model produces an articulate spring bloom extending over the entire longitudinal range of the study area in 2004 (Fig. 5). In the West, where the phytoplankton bloom develops earliest around week 11, CHL-*a* already declines again at the end of the simulation, while the phytoplankton population is still growing in the eastern part of the German Bight. While the timing of the spring bloom is closely matched, its amplitude of around 30 µg l^{-1} east of 6.4° E is slightly underestimated. As in the data, the phase of strong phytoplankton growth initiates shortly after a sharp drop in turbidity from above 3 FTU to 1.5 FTU (Fig. 6). The drop in the light production term (*LPT*) at the end of the bloom period is, however, not linked to turbidity but to low incident irradiances.

Primary production in the model is mostly determined by the availability of light and nutrients. While the distribution of the *LPT* closely resembles the chlorophyll distribution, the nutrient production term (*NPT*) indicates only negligible nutrient limitation throughout most of the simulation period (Fig. 5). The *NPT* only reaches growth-limiting values close to zero west of 6.4° E after week 17. Farther east, nutrients are not yet limiting phytoplankton growth by the end of the simulation period. Zooplankton (not shown) only has a minor impact on the phytoplankton during most of the simulation. Grazing causes, however, the collapse of the phytoplankton bloom after the exhaustion of nutrients in the western part. Since net growth rates under nutrient-depleted conditions are low, phytoplankton then becomes increasingly vulnerable to grazing pressure.

5.4 Bloom advection in 2005

No spatially continuous plankton bloom develops during the first 23 weeks of 2005. Simulated CHL-*a* exceeds 30 µg l^{-1} only in the vicinity of the initial particle position at

5.4° E in late spring. Nonetheless, the patch of elevated CHL-*a* values, extending from the western border of the study area to approximately 6.4° E, is also reproduced by the model, albeit less pronounced than in the measurements.

While the model clearly underestimates enhanced growth rates between week 15 and 18, the temporal dynamics of phytoplankton in the first weeks of the spring bloom is well captured (Fig. 6). In the last weeks of simulation, phytoplankton biomass is still growing when measurements already indicate the collapse of the bloom (week 22–23).

Although light conditions begin to improve between week 12 and 16, they never reach the favourable levels observed in 2004 (Fig. 5). Indeed, the *LPT* even falls back to winter values in the West. In this year, turbidity is clearly determining the light availability while the variability in the incident irradiance is not noticeable in the *LPT*. In contrast to light conditions, nutrient availability does not limit the growth of phytoplankton in spring. As in 2004, a notable impact of zooplankton only occurs in areas of high phytoplankton biomass. Grazing is, thus, strongest near the particle release position in the late phase of the spring bloom.

By resolving the path of single trajectories it is possible to assess the role of hydrodynamics in the spatial division of the study area into a western and an eastern part (Fig. 7). All particles that are located east of 6.3° E after week 15 are initialised with rather low CHL-*a* values during the first weeks of 2005 and stay off the Frisian coast during the entire simulation period. Algal biomass of the majority of these particles does never exceed 7 µg CHL-*a* l^{-1} because low light availability prevents higher productivity (Fig. 5). In contrast, water masses that form the high CHL-*a* patch west of 6.3° E entered the study area during a period of strong eastward drift within only a few days (small circle in Fig. 7). Along with this eastward inflow in week 14, the measured CHL-*a* at the initial position rises severalfold. The trajectories originating during this inflow event later constitute the eastern envelope of the high CHL-*a* patch. Furthermore, they even resemble the characteristic two-tailed shape of the CHL-*a* maximum between 6 and 6.5° E (big grey circle in Fig. 7), which appears in the data between week 18 and 21 (Fig. 5).

To summarise, growth conditions in the study area are rather homogeneous throughout the study area in 2005. The division between high CHL-*a* in the West and significantly lower concentrations in the East can therefore be attributed to a pronounced eastward drift importing high CHL-*a* waters from the adjacent Southern Bight into the western German Bight. To further substantiate the influence of hydrodynamics on the mesoscale bloom structure, the simulation for 2005 is also conducted with 2004 current data (Fig. 8). All other forcings and boundary conditions remain unchanged in this set-up. The result of this model set-up clearly fails to generate the steep CHL-*a* gradients observed in the data. Hydrodynamics in 2004 lack the pronounced inflow that causes the eastward advection of particles with high initial CHL-*a* values far into the central areas of the study area.

6 Discussion

Despite the model's simplicity regarding spatial resolution and ecosystem structure, it is capable of reproducing the general spatio-temporal distribution of CHL-*a* off the Frisian Wadden Sea as measured by the FerryBox on the Cuxhaven – Harwich ferry in 2004 and 2005. More important, our results suggest that different mechanisms – turbidity dynamics and variability of alongshore currents – have led to the observed mesoscale differences in blooming patterns of phytoplankton in the two years of interest.

6.1 Light climate

Typical for phytoplankton in temperate coastal seas, the 2004 spring bloom was triggered by a change in the light climate (Weston et al., 2008; Iriarte and Purdie, 2004; Cloern, 1996). Besides increasing solar irradiances, especially a drop in turbidity greatly improved growth conditions for autotrophs in this year. Turbidity close to estuaries can, in general, be related to winds, tides, and SPM input from rivers (Iriarte and Purdie, 2004; May et al., 2003; Cloern, 1996), but it may also be raised by plank-

tonic organisms in the water column (Tilzer, 1983). It is beyond the scope of this study to explicitly assess the role of different factors in leading to the rapid decrease of turbidity. Weak winds from easterly directions in weeks 15 to 19, however, likely favoured the clearance of the water column (data from Wadden Sea measurement pile, cf. www.coastlab.org). Consequences of ceasing light limitation are accurately predicted by the model, in particular with respect to the spring bloom timing throughout the entire study area. The rapid response of phytoplankton to changes in the available light resource, both in the data as well as in the model, thus, corroborates the pivotal role of SPM in controlling the spring bloom, at least in some years (Tian et al., 2009).

In 2005, the spring bloom developed despite unfavourable light conditions. Instead of a clear water phase, measurements reveal highest turbidity values along with maximum CHL-*a*. Weak temporal and spatial variability in the *LPT* in 2005 cannot account for the observed variability in CHL-*a*. Even strong incident irradiance does not significantly improve the light availability for phytoplankton in highly turbid waters. Phytoplankton blooming is, hence, not always a direct consequence of the local light conditions.

6.2 Hydrodynamics

The phytoplankton distribution in 2005 is clearly controlled by advection underlining the importance of the circulation for modelling ecosystems in highly dynamic coastal seas (Skogen and Moll, 2005). In this case, bloom formation is determined by the simulated eastward inflow of a distinct water mass with elevated CHL-*a* concentration. This is supported by the interpretation of the particle trajectories as well as by the occurrence of high saline water off the West Frisian coast (FerryBox data, not shown). In contrast, water masses that form the CHL-*a* minimum zone east of 6.3° E have resided in coastal waters off the Frisian coast for months experiencing unfavourably light conditions due to high turbidity. The light history of particles is hence distinctively affected by hydrodynamics which in 2005 prevented higher CHL-*a* further east.

The influence of the current pattern is also shown by the artificial alteration of the hydrodynamics in the model. In the 2005 simulation with 2004 hydrodynamics the

spatial CHL-*a* gradient is significantly reduced compared to the reference run.

There is further evidence for the inflow hypothesis from observations of the MERIS satellite described by Petersen et al. (2008): in week 15 a high CHL-*a* area extended from the Rhine estuary to western German Bight waters. Five weeks later, the westward detachment of a large patch of the coastal bloom from the Dutch West Coast indicates the end of eastward inflow. Another two weeks later in week 22, the bloom already decayed in the western German Bight while a huge area of elevated CHL-*a* still persisted offshore in the English Channel.

Hence, hydrodynamic events can bring together water masses with very different histories and biogeochemical signatures and, as a consequence, lead to the development of steep gradients. This mechanism is strong in 2005, leading to an apparent division of the coastal ecosystem in the German Bight into a western and an eastern part. Moreover, our results as well as the FerryBox data demonstrate that steep alongshore gradients may persist in the coastal German Bight despite high current variability.

6.3 Nutrients

Despite the reduction of riverine phosphorus inputs into the southern North Sea in the last decades, high winter values of phosphate and other nutrients still provide favourable conditions for primary producers in the German Bight (Cadée and Hegeman, 2002). The results from 2004 underline the important role of initial, i.e. winter, nutrient concentrations for the spring bloom since the simulated phytoplankton biomass is built up using solely the initial amount of phosphate in the Lagrangian particles. Remineralisation of nutrients through the microbial loop and benthic-pelagic coupling as well as additional nutrient inputs from one of the large rivers discharging into the German Bight are all neglected. We hence suggest that these processes only have a minor importance for algal growth during spring and/or can be compensated by setting a reference CHL:P ratio which is potentially overestimating values during spring. While nutrients are not affecting the timing or the spatial distribution of the spring bloom, phosphate limitation determines its duration in the coastal German Bight in most of

the years (Loebl et al., 2009; Kuipers and van Noort, 2008; van der Zee and Chou, 2005; Skogen et al., 2004). Also the amplitude of the bloom is generally determined by the incipient phosphate concentration. In 2004, the model does, however, not reproduce the observed eastward increase of CHL-*a* concentration, possibly due to the omission of additional nutrient inputs from major rivers (Ems, Weser and Elbe). The crucial role of phosphate motivates the usage of phosphorus as the currency of the ecosystem model. Silicate availability may, however, also become a driving factor as diatoms typically prevail before mass occurrence of *Phaeocystis* (Loebl et al., 2007; Peperzak et al., 1998).

In 2005, and unlike in 2004, nutrient supply remains sufficient during the entire simulation period since the model clearly underestimates phytoplankton growth and, as a consequence, also biomass in the western part of the study area. This also explains the failure of the model to reproduce the termination of the bloom correctly. We suggest that the disagreement is due to an underestimation of phytoplankton light requirements in 2005, possibly pointing at differences in the dominant algal groups in the two years of interest (see below).

6.4 Grazing

Significant grazing on phytoplankton only occurs in the simulation towards the end of the spring bloom. This finding is also supported by Loebl et al. (2007) who observed a strong seasonality of microzooplankton in the coastal German Bight with low grazing pressure in early spring. High zooplankton levels are only hindcasted in the western part of the study area in both years. Here, the bloom starts earlier giving the zooplankton more time to respond to the higher prey availability. Together with decreasing growth rates because of the starting nutrient depletion, zooplankton grazing provokes a steep collapse of CHL-*a* in 2004 within 1–2 weeks. Farther East, both nutrient limitation and zooplankton grazing are still less strong by the end of the simulation in week 20.

In 2005, the inflow of CHL-*a* rich water masses, spatially uniform growth conditions,

and weak grazing can only partly explain the marked alongshore differences in the observed CHL-*a* distribution. The model clearly overestimates CHL-*a* levels in the eastern part of the study area resulting in a less pronounced CHL-*a* gradient. The species distribution of zooplankton in the German Bight is strongly linked to water masses. Martens and Brockmann (1993) and Greve and Reiners (1988) suggest a wave-like spread of zooplankton originating in coastal or estuarine waters. During a winter survey Krause et al. (1995) found a significant eastward increase, i.e. towards less saline or more coastal waters, of zooplankton biomass. Stelfox-Widdicombe et al. (2004) compared microzooplankton at two locations in the Southern Bight of the North Sea during the spring bloom reporting distinctively higher grazing rates at the nearshore station. In the German Bight, a grazing gradient from oceanic to coastal waters may therefore also occur on an alongshore axis towards the estuaries of Elbe, Weser and, the Jade bay, along with the rising influence of estuarine water.

On the base of these findings, we suppose that the abrupt change of CHL-*a* in 2005, which is caused by the convergence of different water masses, may also be reflected in spatial heterogeneity of the zooplankton community, which is not resembled by the model. An important, yet often overlooked, factor that temporarily enhances grazing in nearshore waters is the mass occurrence of meroplanktonic larvae of benthic invertebrates, which mostly originate in the adjacent intertidal Wadden Sea and can be therefore associated with low saline water masses (Brandt et al., 2008; Martens and Brockmann, 1993). Unlike other zooplankton groups, meroplanktonic larvae can appear in high abundances without a preceding phytoplankton bloom since their occurrence is solely depending on spawning. Smetacek and Cloern (2008) support this argument by recently stating that meroplankton has the potential to significantly influence lower trophic levels in coastal ecosystems like the German Bight.

6.5 Algal community structure and stoichiometry

Despite the general agreement with observations, the model results lack few features inherent to the data. The simulated phytoplankton growth, for example, is slower during

the first weeks of the spring bloom than the measurements suggest in 2004. This mismatch is partly due to specific model formulations. The multiplication of terms in the formulation of the primary production (Eq. 1) clearly leads to a conservative estimate compared to other approaches (e.g. the Liebig law of the minimum or temperature independence of the initial slope of the P/I-curve Geider et al., 1998).

Another origin of model errors can be linked to simplifications in the ecosystem model that completely neglects the intrinsic variability of all considered compartments (i.e. nutrients, algae and herbivores). Wirtz and Eckhardt (1996) have shown the critical relevance of variable traits in modelling multi-species phytoplankton communities. Intracellular element ratios are key variables of algal physiology, which also critically affect all model–data comparisons. Keeping CHL:C and C:P constant is, thus, not consistent with known variations in phytoplankton stoichiometry and introduces significant uncertainty. Deviations in the observed range between simulated and measured data are even much smaller than the reported range of variability of the two stoichiometric ratios (Llewellyn et al., 2005; Hecky and Kilham, 1988; Geider, 1987; Tett et al., 1985). Much of the unexplained deviations between model and data could be, thus, mainly attributed to errors linked to fixed intracellular element ratios. That is, the consideration of variable intracellular element ratios appears essential to simulate the steepness of the observed gradients. In fact, measurements in the English Channel (Llewellyn et al., 2005) and Helgoland Roads (Wiltshire, unpublished) indicate the strong variability in CHL:C and it is an ongoing effort to represent the underlying mechanisms causing these fluctuations (Pahlow, 2005).

Another important and variable trait for this study is the optimal irradiance I_{opt} (Macedo et al., 2001). Changing photosynthetic characteristics do not only matter when simulating the course of a bloom, but may also be relevant for understanding interannual differences. In 2005, the underestimation of CHL-*a* in the western part can be attributed to an overrated light limitation that is caused by the selection of a too large I_{opt}. It appears therefore likely that diatoms, which have lower light requirements, e.g. a lower I_{opt}, than *Phaeocystis*, dominated the spring bloom in this year (cf. Wiltshire et al.,

2008). Observations in the Dutch Wadden Sea in 2004, however, identified *Phaeocystis* to be the dominating species during April (Kuipers and van Noort, 2008). Higher numbers of diatoms were only observed thereafter in May. It is likely that *Phaeocystis* was able to outcompete diatoms already early in 2004 because of the exceptionally high light availability after week 12.

6.6 1-D Lagrangian modelling

The simplified approach of using moving particles along a one-dimensional projection entails several advantages: First, the transect matches the two adjacent ferry routes, so that the availability and reliability of physical forcing data and fluorescence measurements. This is particularly important as results indicate that mesoscale variability may originate from high-frequent fluctuations of ambient conditions. Of course, an extrapolation of simulated values to a larger area beyond the transect would require a different approach.

Advantages of the Lagrangian over the more common Eulerian approach for this study comprise the ability to preserve strong gradients and the possibility to easily assess the particle history. Furthermore, the one-dimensional approach entails a greatly reduced computational effort compared to higher-dimensional set-ups, facilitating parameter calibration and sensitivity studies (Soetaert and Middelburg, 2008).

7 Conclusions

The study identified two different mechanisms explaining the observed spring dynamics of phytoplankton in a coastal marine ecosystem. In 2004 the buildup of CHL-*a* is determined by short term variability in turbidity. In contrast, detailed knowledge of the history of individual water masses is essential to understand the phytoplankton dynamics in 2005. Under severe light limitation due to high turbidity, the bloom has to be triggered by the import of water masses containing higher phytoplankton concentrations. In ad-

dition, spatial variability of zooplankton grazing with higher impact in coastal waters is probably enhancing the horizontal gradients in spring. Reducing the uncertainties regarding the variability of intracellular element ratios presents a major challenge to further improve the understanding of observed CHL-*a* gradients in the future.

The successful simulation of fundamentally different spring bloom dynamics in two consecutive years with constant parameters demonstrates the appropriateness of this simple coupled model for analysing the origin of mesoscale CHL-*a* patterns in spring blooms. Against the common trend of building ever more complex models, the reduction of hydrodynamic information to a lowpass filtered horizontal transect facilitates the understanding of mesoscale structures along the shore. The availability of high-frequent FerryBox data has thereby proven to be paramount. In this context, the attempt to reproduce time-series data of dynamic coastal systems without taking into account horizontal transport appears to be at least difficult. A satisfying correlation between ecosystem dynamics and local conditions in one period does not guarantee its validity in other time intervals. It remains surprising, however, that the reproduction of alongshore variability is relatively successful despite the ignorance of cross-shore processes and turbulent diffusion in this tidally-dominated coastal sea.

Though our coupled Lagrangian ecosystem model is able to simulate the basic dynamics of the plankton community, it is obviously limited to the winter and spring period. Many assumptions, e.g. the ignorance of remineralisation processes or adaptation in algal stoichiometry and/or community structure, have to be re-considered prior to a potential application to the entire season. Our study also points to the relevance of time-continuous as well as spatially explicit data of herbivores including microzooplankton. A combination of operational FerryBox and CPR measurements would be, thus, an important step towards an effective characterisation of ecosystem dynamics in a regional shelf sea like the North Sea.

Appendix A

Data integration

The considered FerryBox variables were measured by the following devices (analyser, manufacturer, country): Temperature T [°C] (PT100, FSI, USA), turbidity Tb [FTU] (CUS31W2A, Endress & Hauser, Germany), and chlorophyll-a (CHL-a) [$\mu g\,l^{-1}$] (SCUFA-II, Turner Design, USA). All measured data are binned in time and space with a bin size of 7d and 0.2° to eliminate high frequency fluctuations and to fill smaller data gaps. By interpolating these coarse distributions to a higher resolution grid with a bin size of 1d and 0.02° smooth and consistent distributions are generated (Fig. 5). Data gaps are filled with the nearest available value in time dimension, since a failure of a measurement device normally leads to missing data along the entire spatial domain.

Irradiance data are composed from pile data recorded at 7.47° E, 53.71° N in the Wadden Sea during spring and summer (source: www.coastlab.org) and synthetic values derived with the astronomic method described by Ebenhöh et al. (1997) for data gaps, which occur mainly in winter when the pile is not operating. Phosphate was measured in filtered surface water 4 and 10 km off the Dutch coast (5.10° E, 53.46° N and 5.15° E, 53.41° E) approximately once a month (source: database DONAR operated by the Dutch Ministry of Transport, Public Works and Water Management, www.waterbase.nl).

A1 Model architecture

The linear regression of vertically integrated, mean daily currents produced by a 3 nm set-up of the General Estaurine Transport Model (GETM) reveals a significant correlation between their zonal and the meridional components (u and v) in the vicinity of the ferry route (2004: Pearson r=0.86, p<0.01, 2005: r=0.81, p<0.01, vertically integrated daily mean currents during the first 140 days of the respective year, Fig. 1). Hence, daily mean currents are directed either to the Northeast or to the Southwest.

BGD
6, 4993–5030, 2009

The reliability of this projection, however, declines outside the range of 5.2° E and 7.5° E where the correlation is calculated. The particle tracking algorithm uses the mean daily zonal velocity component u generated by GETM to compute the meridional velocity component v

$$v = a \times u + b \tag{A1}$$

with the parameter values a=0.349 and b=0.003 m×s^{-1} derived by linear regression (first 140d of both years). In the following, b is neglected for its smallness. The current velocity w along the model domain at position x and time t is hence solely a function of u and given by

$$w(t,x) = \sqrt{u^2(t,x) + v^2(t,x)} \tag{A2}$$

$$= \sqrt{1 + a^2} \times u(t,x) \tag{A3}$$

resulting in the change of position of particle i

$$dx(t,x_i) = w(t,x_i) \times dt\,. \tag{A4}$$

An explicit fifth-order Runge-Kutta algorithm is applied to integrate Eq. (A4).

A2 Ecosystem model

P_P denotes the primary production of phytoplankton

$$P_P = \mu_P \times \overbrace{\epsilon_P}^{\text{Temperature}} \times \frac{\overbrace{N}^{\text{Nutrients}}}{N + k_N} \times \overbrace{\frac{1}{k_z \times \zeta} \times \int_{x_D}^{x_0} \frac{4}{1 + 4 \times x}\, dx}^{\text{Light}} \times P \tag{A5}$$

BGD
6, 4993–5030, 2009

with the maximum growth rate μ_p, the half saturation constant for nutrient uptake k_N, the light attenuation coefficient k_z, and the water depth ζ. The labelled terms in Eq. (A5) are the dimensionless terms for the nutrient production (NPT) and the light production (LPT) and the temperature production (TPT). Following Ebenhöh et al. (1997), the depth integral of the *p/I*-curve is dimensionless with

$$x_0 = \frac{I_0}{I_{\text{opt}} \times \epsilon_P} \tag{A6}$$

$$x_D = \frac{I_D}{I_{\text{opt}} \times \epsilon_P} \tag{A7}$$

where I_0 and I_D are the photosynthetically active radiation (PAR) at the surface and the bottom, respectively. PAR is assumed to be a constant fraction r_{PAR}=0.5 of the incident irradiance (Ebenhöh et al., 1997). The corresponding *p/I*-curve is a Monod function with the scaling parameter I_{opt}.

All biological processes depend exponentially on the water temperature T

$$\epsilon_X = Q_{10,X}^{(T-T_0)/10}, \tag{A8}$$

with $Q_{10,X}$ determining the sensitivity to changes in T and the temperature T_0 at which ϵ_X=1. The subscript X stands for either P (phytoplankton) or Z (zooplankton).

Observational evidence supports the use of a Holling-type III functional response to simulate the zooplankton grazing P_Z on phytoplankton (Gentleman et al., 2003; Verity, 1991).

$$P_Z = \epsilon_Z \times \mu_Z \times \frac{P^2}{P^2 + k_P^2} \times Z, \tag{A9}$$

with μ_Z and k_P indicating the specific growth rate and the half saturation constant for grazing, respectively.

A3 Initial conditions and forcing

The surface PAR I_0 is regarded spatially uniform. Turbidity is a relative quantity that can be related to the diffuse light attenuation coefficient k_Z. This relationship is, however, variable and should be ideally established empirically (Davies-Colley and Smith, 2001). Here, it is estimated as

$$k_Z = a \times Tb + b \tag{A10}$$

with the parameters a=0.15 $m^{-1} \times FTU^{-1}$ and b=0.05 m^{-1}.

We assume that the initial value for the zooplankton concentration is a fraction r_Z of phytoplankton biomass P at the time $t_0 - \tau_Z$

$$Z(t_0, x_0) = \max(Z_{\min}, P(t_0 - \tau_Z, x_0) \times r_Z), \tag{A11}$$

where $Z_{\min}$ and τ_Z are the minimum zooplankton biomass and time lag for zooplankton, respectively.

Acknowledgements. We thank F. Schroeder and W. Petersen for providing FerryBox data, J. Staneva for the hydrodynamic data from GETM and G. Flöser for the irradiance data from the GKSS measurement pile.

References

Ainsworth, C.: Oceanography: FerryBoxes Begin to Make Waves, Science, 322, 1627–1629, 2008. 4996

Beddig, S., Brockmann, U., Dannecker, W., Körner, D., Pohlmann, T., Puls, W., Radach, G., Rebers, A., Rick, H. J., Schatzmann, M., et al.: Nitrogen fluxes in the German Bight, Mar. Pollut. Bull., 34, 382–394, 1997. 4997

Brandt, G., Wehrmann, A., and Wirtz, K. W.: Rapid invasion of *Crassostrea gigas* into the German Wadden Sea dominated by larval supply, J. Sea Res., 59, 279–296, 2008. 5009

Cadée, G. C. and Hegeman, J.: Phytoplankton in the Marsdiep at the end of the 20th century; 30 years monitoring biomass, primary production, and Phaeocystis blooms, J. Sea Res., 48, 97–110, 2002. 5007

Cloern, J. E.: An empirical model of the phytoplankton chlorophyll:carbon ratio– the conversion factor between productivity and growth rate, Limnol. Oceanogr., 40, 1313–1321, 1995. 5000, 5022

Cloern, J. E.: Phytoplankton bloom dynamics in coastal ecosystems: A review with some general lessons from sustained investigation of San Francisco Bay, California, Rev. Geophys., 34, 127–168, 1996. 4995, 5005

Davies-Colley, R. J. and Smith, D. G.: Turbidity, suspended sediment, and water clarity: A review , J. Am. Water. Resour. As., 37, 1085–1101, 2001. 5016

Devlin, M. J., Barry, J., Mills, D. K., Gowen, R. J., Foden, J., Sivyer, D., and Tett, P.: Relationships between suspended particulate material, light attenuation and Secchi depth in UK marine waters, Estuar., Coast. and Shelf Sci., 79, 429–439, 2008. 5022

Ebenhöh, W., Baretta-Bekker, J. G., and Baretta, J. W.: The primary production model in the ecosystem model ERSEM II, J. Sea Res., 38, 173–192, 1997. 4999, 5013, 5015, 5022

Elser, J., Sterner, R., Galford, A., Chrzanowski, T., Findlay, D., Mills, K., Paterson, M., Stainton, M., and Schindler, D.: Pelagic C:N:P stoichiometry in a eutrophied lake: responses to a whole-lake food-web manipulation, Ecosystems, 3, 293–307, 2000. 5000

Faure, V., Pinazo, C., Torréton, J. P., and Douillet, P.: Relevance of various formulations of phytoplankton chlorophyll-*a*: carbon ratio in a 3D marine ecosystem model, C. R. Biologies, 329, 813–822, 2006. 5022

Furnas, M. J.: In situ growth rates of marine phytoplankton: approaches to measurement, community and species growth rates, J. Plankton. Res., 12, 1117–1151, 1990. 5022

Geider, R. J.: Light and temperature depenence of the carbon to chlorophyll-*a* ratio in microalgae and cyanobacteria: implications for physiology and growth of phytoplankton, New Phytol., 106, 1–34, 1987. 5000, 5010, 5022

Geider, R. J., MacIntyre, H. L., and Kana, T. M.: A dynamic regulatory model of phytoplanktonic acclimation to light, nutrients, and temperature, Limnol. Oceanogr., 43, 679–694, 1998. 5010

Gentleman, W., Leising, A., Frost, B., Strom, S., and Murray, J.: Functional responses for zooplankton feeding on multiple resources: a review of assumptions and biological dynamics, Deep-Sea Res. Part II, 50, 2847–2875, 2003. 5015

Greve, W. and Reiners, F.: Plankton timespace dynamics in German Bight–a systems approach, Oecologia, 77, 487–496, 1988. 5009

Greve, W., Reiners, F., Nast, J., and Hoffmann, S.: Helgoland Roads meso- and macrozooplankton time-series 1974 to 2004: lessons from 30 years of single spot, high frequency

sampling at the only off-shore island of the North Sea, Helgol. Mar. Res., 58, 274–288, 2004. 5000
Hansen, P. J., Bjornsen, P. K., and Hansen, B. W.: Zooplankton grazing and growth: Scaling within the 2–2000 μm body size range, Limnol. Oceanogr., 42, 687–704, 1997. 5022
Hecky, R. E. and Kilham, P.: Nutrient limitation of phytoplankton in freshwater and marine environments: A review of recent evidence on the effects of enrichment., Limnol. Oceanogr., 33, 796–822, 1988. 5010
Iriarte, A. and Purdie, D. A.: Factors controlling the timing of major spring bloom events in an UK south coast estuary, Estuar., Coast. and Shelf Sci., 61, 679–690, 2004. 4995, 4997, 5005
Joint, I. and Pomroy, A.: Phytoplankton biomass and production in the southern North Sea, Mar. Ecol. Prog. Ser., 99, 169–169, 1993. 4999
Klausmeier, C., Litchman, E., and Levin, S.: Phytoplankton growth and stoichiometry under multiple nutrient limitation, Limnol. Oceanogr., 49, 1463–1470, 2004. 5000
Krause, M., Dippner, J. W., and Beil, J.: A review of hydrographic controls on the distribution of zooplankton biomass and species in the North Sea with particular reference to a survey conducted in January–March 1987, Prog. Oceanogr., 35, 81–152, 1995. 5009
Kuipers, B. R. and van Noort, G. J.: Towards a natural Wadden Sea?, J. Sea Res., 60, 44–53, 2008. 5008, 5011
Lacroix, G., Ruddick, K., Park, Y., Gypens, N., and Lancelot, C.: Validation of the 3D biogeochemical model MIRO&CO with field nutrient and phytoplankton data and MERIS-derived surface chlorophyll-*a* images, J. Mar. Syst., 64, 66–88, 2007. 4996
Levin, S.: The problem of pattern and scale in ecology: the Robert H. MacArthur award lecture, Ecology, 73, 1943–1967, 1992. 4996
Llewellyn, C. A., Fishwick, J. R., and Blackford, J.: Phytoplankton community assemblage in the English Channel: a comparison using chlorophyll-*a* derived from HPLC-CHEMTAX and carbon derived from microscopy cell counts, J. Plankton. Res., 27, 103–119, 2005. 5000, 5010, 5022
Loebl, M., Dolch, T., and van Beusekom, J. E. E.: Annual dynamics of pelagic primary production and respiration in a shallow coastal basin, J. Sea Res., 58, 269–282, 2007. 5008
Loebl, M., Colijn, F., van Beusekom, J. E. E., Baretta-Bekker, J. G., Lancelot, C., Philippart, C. J. M., Rousseau, V., and Wiltshire, K. H.: Recent patterns in potential phytoplankton limitation along the Northwest European continental coast, J. Sea Res., 61, 34–43, 2009.

4995, 4997, 5008
Lucas, L., Koseff, J., Cloern, J., Monismith, S., and Thompson, J.: Processes governing phytoplankton blooms in estuaries. I: The local production-loss balance, Mar. Ecol. Prog. Ser., 187, 1–15, 1999a. 4995
Lucas, L., Koseff, J., Monismith, S., Cloern, J., and Thompson, J.: Processes governing phytoplankton blooms in estuaries 2: The role of horizontal transport, Mar. Ecol. Prog. Ser., 187, 17–30, 1999b. 4995
Lucas, L., Koseff, J., Monismith, S., and Thompson, J.: Shallow water processes govern system-wide phytoplankton bloom dynamics: A modeling study, J. Mar. Syst., 75, 70–86, 2009. 4995
Macedo, M. F., Duarte, P., Mendes, P., and Ferreira, J. G.: Annual variation of environmental variables, phytoplankton species composition and photosynthetic parameters in a coastal lagoon, 2001. 5010
Martens, P. and Brockmann, U.: Different zooplankton structures in the German Bight, Helgol. Mar. Res., 47, 193–212, 1993. 5009
Martin, A.: Phytoplankton patchiness: the role of lateral stirring and mixing, Prog. Oceanogr., 57, 125–174, 2003. 4995
May, C. L., Koseff, J. R., Lucas, L. V., Cloern, J. E., and Schoellhamer, D. H.: Effects of spatial and temporal variability of turbidity on phytoplankton blooms, Mar. Ecol. Prog. Ser., 254, 111–128, 2003. 5005
Muylaert, K., Gonzales, R., Franck, M., Lionard, M., Van der Zee, C., Cattrijsse, A., Sabbe, K., Chou, L., and Vyverman, W.: Spatial variation in phytoplankton dynamics in the Belgian coastal zone of the North Sea studied by microscopy, HPLC-CHEMTAX and underway fluorescence recordings, J. Sea Res., 55, 253–265, 2006. 4995
Pahlow, M.: Linking chlorophyll-nutrient dynamics to the Redfield N:C ratio with a model of optimal phytoplankton growth, Mar. Ecol. Prog. Ser., 287, 33–43, 2005. 5010
Peperzak, L., Colijn, F., Gieskes, W. W. C., and Peeters, J. C. H.: Development of the diatom-Phaeocystis spring bloom in the Dutch coastal zone of the North Sea: the silicon depletion versus the daily irradiance threshold hypothesis, J. Plankton. Res., 20, 517–537, 1998. 5008
Petersen, W., Petschatnikov, M., Schroeder, F., and Colijn, F.: FerryBox systems for monitoring coastal waters, in: Building the European Capacity in Operational Oceanography: Proc. Third International Conference on EuroGOOS, Elsevier Oceanography Series Publication series, edited by Dahlien, H., Flemming, N. C., Knittis, K., and Petersson, S. E., 19, 325–

333, 2003. 4998
Petersen, W., Wehde, H., Krasemann, H., Colijn, F., and Schroeder, F.: FerryBox and MERIS – Assessment of coastal and shelf sea ecosystems by combining in situ and remotely sensed data, Estuar., Coast. and Shelf Sci., 77, 296–307, 2008. 4996, 4998, 5007
Prins, T., Smaal, A., Pouwer, A., and Dankers, N.: Filtration and resuspension of particulate matter and phytoplankton on an intertidal mussel bed in the Oosterschelde estuary (SW Netherlands), Mar. Ecol. Prog. Ser., 142, 121–134, 1996. 4995
Radach, G.: Ecosystem functioning in the German Bight under continental nutrient inputs by rivers, Estuaries Coasts, 15, 477–496, 1992. 4997
Raven, J. A. and Geider, R. J.: Temperature and algal growth, New. Phytol., 110, 441–461, 1988. 5022
Siegismund, F. and Schrum, C.: Decadal changes in the wind forcing over the North Sea, Climate Res., 18, 39–45, 2001. 4997
Skogen, M. D. and Moll, A.: Importance of ocean circulation in ecological modeling: An example from the North Sea, J. Mar. Syst., 57, 289–300, 2005. 5006
Skogen, M. D., Søiland, H., and Svendsen, E.: Effects of changing nutrient loads to the North Sea, J. Mar. Syst., 46, 2004. 5008
Smetacek, V. and Cloern, J. E.: Oceans: On Phytoplankton Trends, Science, 319, 1346–1348, 2008. 5009
Soetaert, A. F. H. K. and Middelburg, J. J.: Present nitrogen and carbon dynamics in the Scheldt estuary using a novel 1-D model, Biogeosciences, 5, 981–1006, 2008, http://www.biogeosciences.net/5/981/2008/. 5011
Sommer, U.: Biologische Meereskunde, Springer, 1998. 4994
Staneva, J., Stanev, E. V., Wolff, J. O., Badewien, T., Reuter, R., Flemming, B., Bartholomä, and Bolding, K.: Hydrodynamics and sediment dynamics in the German Bight. A focus on observations and numerical modelling in the East Frisian Sea, Cont. Shelf. Res., 29, 302–319, 2009. 4997, 4998
Stelfox-Widdicombe, C. E., Archer, S. D., Burkill, P. H., and Stefels, J.: Microzooplankton grazing in Phaeocystis and diatom-dominated waters in the southern North Sea in spring, J. Sea Res., 51, 37–51, 2004. 5009, 5022
Stips, A., Bolding, K., Pohlmann, T., and Burchard, H.: Simulating the temporal and spatial dynamics of the North Sea using the new model GETM (General Estuarine Transport Model), Ocean Dynam., 54, 266–283, 2004. 4998

Taylor, A. H., Geider, R. J., and Gilbert, F. J. H.: Seasonal and latitudinal dependencies of phytoplankton carbon-to-chlorophyll-*a* ratios: results of a modelling study, Mar. Ecol. Prog. Ser., 152, 51–66, 1997. 5000

Tett, P., Heaney, S. I., and Droop, M. R.: The redfield ratio and phytoplankton growth rate., J. Mar. Biol. Assoc. UK, 65, 487–504, 1985. 5010

Thomas, A., Townsend, D., and Weatherbee, R.: Satellite-measured phytoplankton variability in the Gulf of Maine, Cont. Shelf. Res., 23, 971–989, 2003. 4995

Tian, T., Merico, A., Su, J., Staneva, J., Wiltshire, K., and Wirtz, K.: Importance of resuspended sediment dynamics for the phytoplankton spring bloom in a coastal marine ecosystem, J. Sea Res., in press, doi:10.1016/j.seares.2009.04.001, 2009. 4996, 5006

Tilzer, M. M.: The importance of fractional light absorption by photosynthetic pigments for phytoplankton productivity in Lake Constance., Limnol. Oceanogr., 28, 833–846, 1983. 5006

Townsend, D., Cammen, L., Holligan, P., Campbell, D., and Pettigrew, N.: Causes and consequences of variability in the timing of spring phytoplankton blooms, Deep-Sea Res. I, 41, 747–765, 1994. 4995

van der Zee, C. and Chou, L.: Seasonal cycling of phosphorus in the Southern Bight of the North Sea, Biogeosciences, 2, 27–42, 2005, http://www.biogeosciences.net/2/27/2005/. 5008

Verity, P. G.: Measurement and simulation of prey uptake by marine planktonic ciliates fed plastidic and aplastidic nanoplankton., Limnol. Oceanogr., 36, 729–750, 1991. 5015

Weston, K., Greenwood, N., Fernand, L., Pearce, D. J., and Sivyer, D. B.: Environmental controls on phytoplankton community composition in the Thames plume, UK, J. Sea Res., 60, 262–270, 2008. 5005

Wiltshire, K. H. and Manly, B. F. J.: The warming trend at Helgoland Roads, North Sea: phytoplankton response, Helgol. Mar. Res., 58, 269–273, 2004. 4997

Wiltshire, K. H., Malzahn, A. M., Wirtz, K. W., Greve, W., Janisch, S., Mangelsdorf, P., Manly, B. F. J., and Boersma, M.: Resilience of North Sea phytoplankton spring bloom dynamics: An analysis of long-term data at Helgoland Roads, Limnol. Oceanogr., 53, 1294–1302, 2008. 4997, 5010

Wirtz, K. W. and Eckhardt, B.: Effective variables in ecosystem models with an application to phytoplankton succession, Ecol. Model., 92, 33–53, 1996. 5010

Woods, J., Perilli, A., and Barkmann, W.: Stability and predictability of a virtual plankton ecosystem created with an individual-based model, Prog. Oceanogr., 67, 43–83, 2005. 4997

Table 1. Model parameters and their values (see also Appendix).

Symbol	Definition	Value	Unit	Ref.
a	Light extinction parameter	0.15	$[m^{-1} \times FTU^{-1}]$	Devlin et al. (2008)
b	Extinction offset	0.05	$[m^{-1}]$	Devlin et al. (2008)
β	Zooplankton assimilation efficiency	0.5	[ ]	
I_{opt}	Scaling parameter of the *p/I*-curve	225	$[W \times m^{-2}]$	Ebenhöh et al. (1997)
C:P	Carbon to phosphorus ratio	106	$[mol\,C \times (mol\,P)^{-1}]$	Redfield ratio
CHL:C	CHL-*a* to carbon ratio	0.3	$[g\,CHL\text{-}a \times (mol\,C)^{-1}]$	Faure et al. (2006) Llewellyn et al. (2005) Geider (1987)
k_N	Half-saturation of nutrient limitation	0.5	$[\mu mol\,P \times l^{-1}]$	
k_P	Half-saturation of grazing	0.75	$[\mu mol\,P \times l^{-1}]$	
μ_p	Phytoplankton maximum growth rate	0.69	$[d^{-1}]$	Cloern (1995); Furnas (1990)
μ_z	Zooplankton maximum growth rate	0.56	$[d^{-1}]$	Stelfox-Widdicombe et al. (2004)
$Q_{10,P}$	Temperature sensitivity zooplankton	3.0	[ ]	Raven and Geider (1988)
$Q_{10,Z}$	Temperature sensitivity phytoplankton	2.0	[ ]	Hansen et al. (1997)
r_{PAR}	Ratio between incident irradiance and PAR	0.5		Ebenhöh et al. (1997)
r_Z	Initial zooplankton fraction	0.04	[ ]	
τ_Z	Time lag for zooplankton initialisation	14	[d]	
T_0	Reference temperature	10	[°C]	
Z_{min}	Minimum zooplankton biomass	0.0075	$[\mu mol\,P \times l^{-1}]$	

BGD
6, 4993–5030, 2009

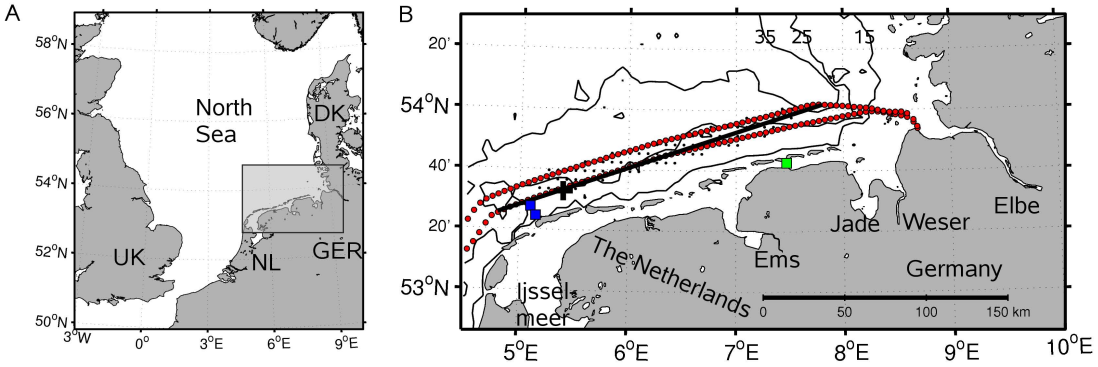

Fig. 1. (A) North Sea region including the study area (boxed). **(B)** Study area with the FerryBox route (red dots), the model transect (black line) and the release positions of the particles (black cross) at 5.4° E. Black dots indicate General Estuarine Transport Model (GETM) grid points used in the current analysis (see Fig. 3). Coastal measurement pile (green square), nutrient measurement stations (blue squares) and depth contours (15, 25 and 35 m).

BGD
6, 4993–5030, 2009

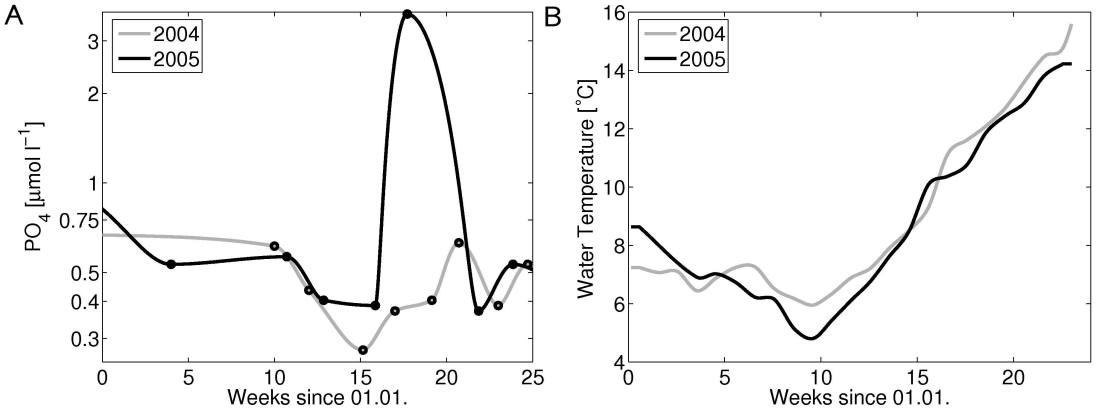

Fig. 2. (A) Phosphate in filtered surface water as the mean of measurements at two stations off the Dutch coast (5.10° E, 53.46° N and 5.15° E, 53.41° E, Fig. 1) in 2004 (grey line) and 2005 (black line) (source: DONAR database operated by the Dutch Ministry of Transport, Public Works and Water Management). **(B)** Weekly mean water temperature, averaged between 5 and 8° E measured by the FerryBox in 2004 (grey line) and 2005 (black line).

BGD
6, 4993–5030, 2009

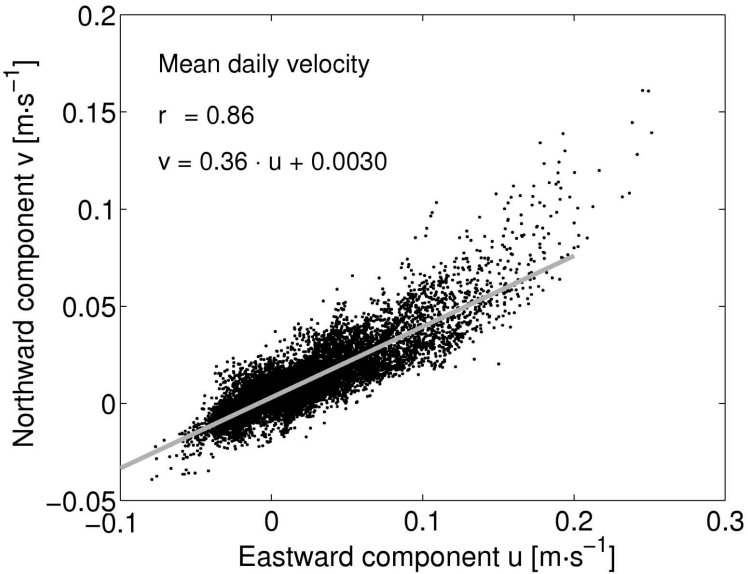

Fig. 3. Mean daily current components near the ferry route calculated by the General Estuarine Transport Model (GETM) for the first 20 weeks in 2004. Considered GETM grid points are indicated as black dots in Fig. 1.

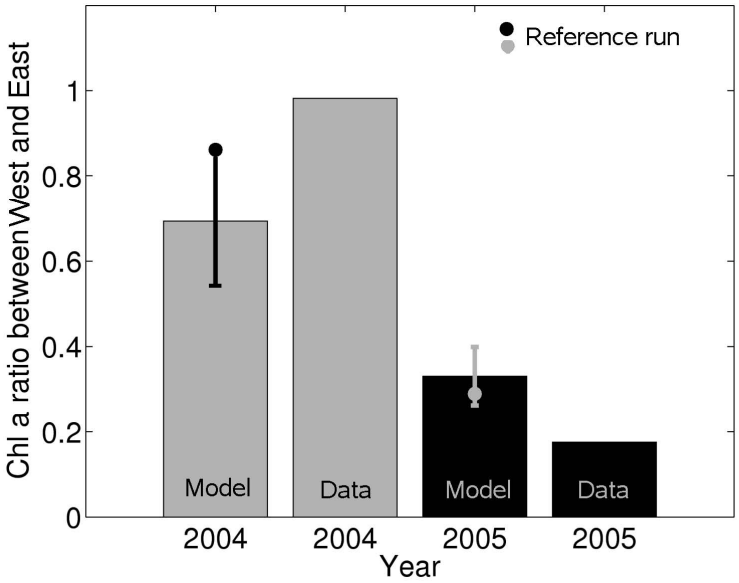

Fig. 4. Sensitivity of model results to the systematic variation of four parameters (I_{opt}[125 ... 225 W×m^{-2}], k_N[0.3 ... 0.7 µmol P×l^{-1}], k_P[0.25 ... 0.9 µmol P×l^{-1}] and Z_{min}[0.0075 ... 0.015 µmol P×l^{-1}]) regarding the zonal gradient in CHL-*a*. The gradient is expressed as the ratio of mean CHL-*a* concentrations in two adjacent areas as shown in Fig. 5. Values below one indicate higher CHL-*a* in the West than in the East. Errorbars show the standard deviation of a total of 162 model runs, solid circles denote the ratios of the reference run. Data bars display the same ratio derived from FerryBox measurements.

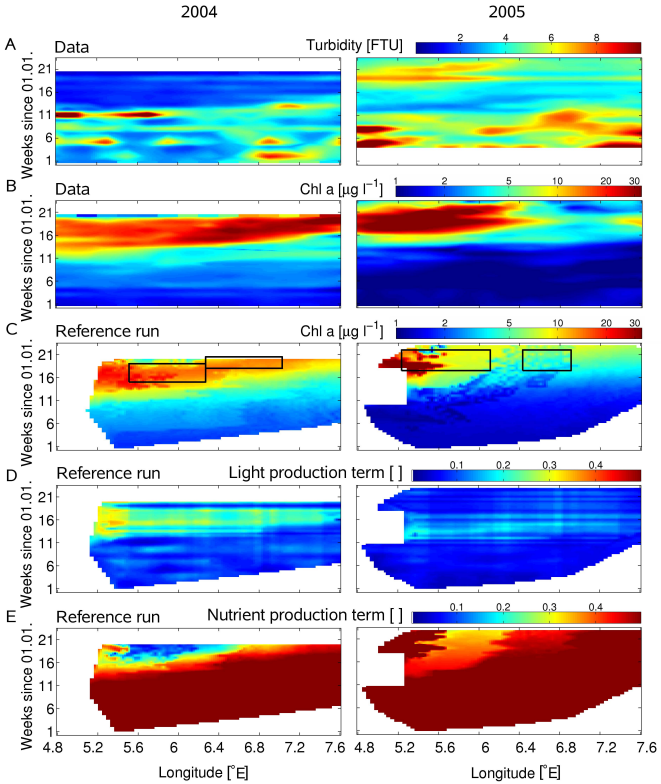

Fig. 5. **(A)** Turbidity measured by the FerryBox between Cuxhaven, Germany and Harwich, UK in 2004 and 2005 (Fig. 1); See Appendix for more details on data treatment. **(B)** CHL-*a* measured by the FerryBox (cf. A). **(C)** Simulated CHL-*a* concentration; squares indicate areas that are used to calculate the CHL-*a* gradient for the sensitivity study (see Sect. 3 for more details); the data gap at the western edge in 2005 is due to missing particle coverage. **(D)** Simulated light production term (Eqs. 1, A5). **(E)** Simulated nutrient production term (Eqs. 1, A5).

BGD
6, 4993–5030, 2009

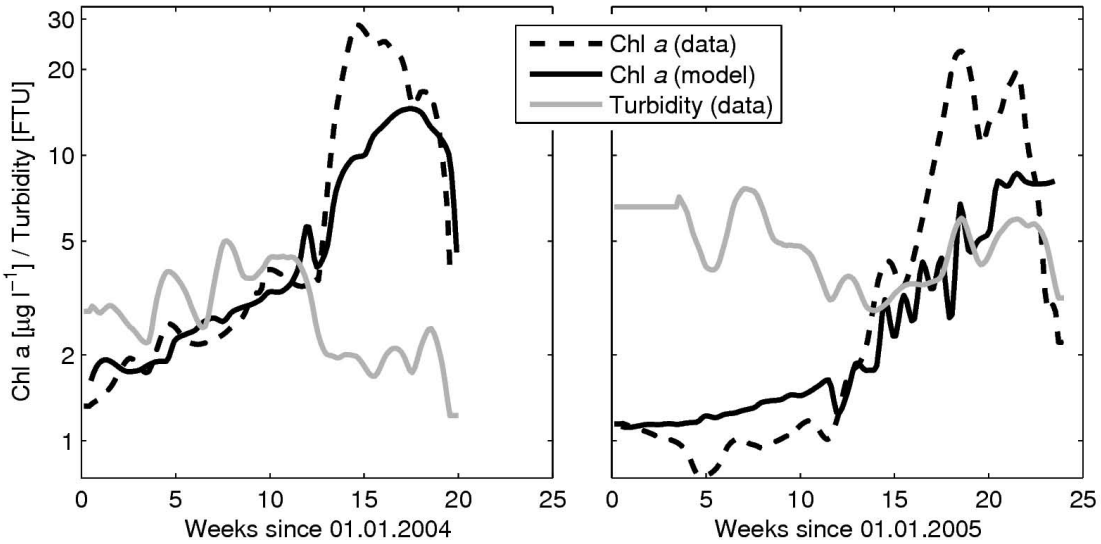

Fig. 6. Measured (black dashed) and simulated (black solid) CHL-*a* and measured turbidity (grey) at 6.2° E.

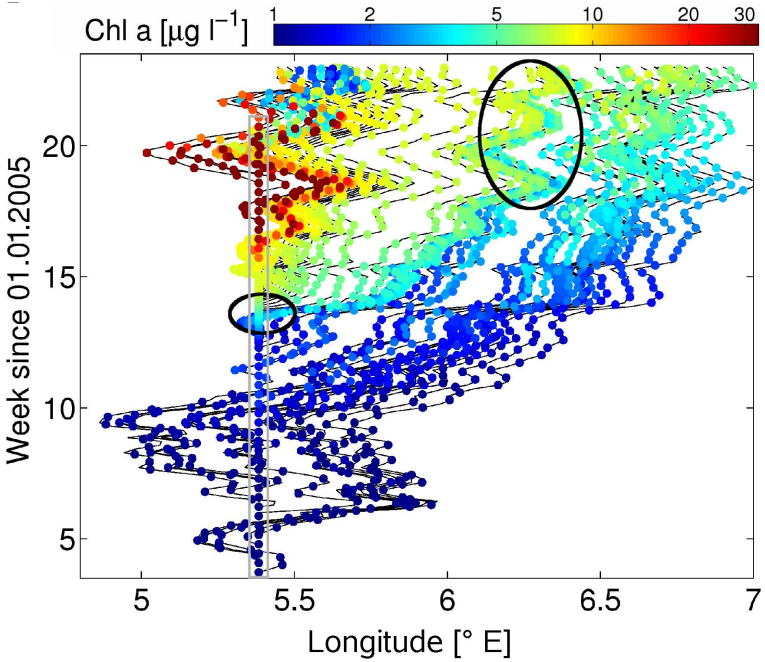

Fig. 7. Model trajectories coloured according to their simulated CHL-*a* values; all particles are released at 5.4° E. The small ellipse marks the eastward inflow of a water mass with elevated chlorophyll-*a* concentrations; the big grey circle indicates the fate of the first particles released within the small circle that later in the spring bloom form the border between a high and a low CHL-*a* region.

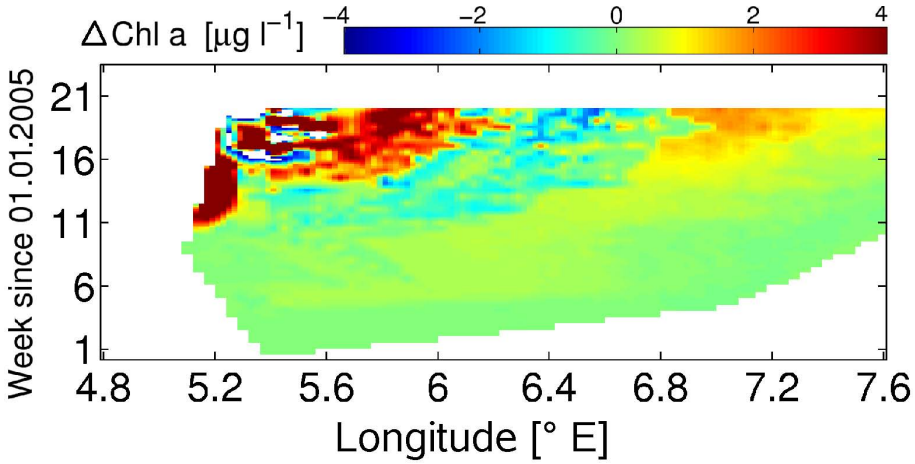

Fig. 8. Differences in CHL-*a* between the reference run in 2005 and the same run with 2004 hydrodynamics. Deviations are only attributable to differences in the current system.